Effect of chemistry and turbulence on NO formation in oxygen-natural gas flames

By J.-M. Samaniego[1], F. N. Egolfopoulos[2] AND C. T. Bowman[3]

The effects of chemistry and turbulence on NO formation in oxygen-natural turbulent diffusion flames gas flames have been investigated. The chemistry of nitric oxides has been studied numerically in the counterflow configuration. Systematic calculations with the GRI 2.11 mechanism for combustion of methane and NO chemistry were conducted to provide a base case. It was shown that the 'simple' Zeldovich mechanism accounts for more than 75% of N_2 consumption in the flame in a range of strain-rates varying between 10 and 1000 s^{-1}. The main shortcomings of this mechanism are: 1) overestimation (15%) of the NO production rate at low strain-rates because it does not capture the reburn due to the hydrocarbon chemistry, and 2) underestimation (25%) of the NO production rate at high strain-rates because it ignores NO production through the prompt mechanism. Reburn through the Zeldovich mechanism alone proves to be significant at low strain-rates. A one-step model based on the Zeldovich mechanism and including reburn has been developed. It shows good agreement with the GRI mechanism at low strain-rates but underestimates significantly N_2 consumption (about 50%) at high strain-rates. The role of turbulence has been assessed by using an existing 3-D DNS data base of a diffusion flame in decaying turbulence. Two PDF closure models used in practical industrial codes for turbulent NO formation have been tested. A simpler version of the global one-step chemical scheme for NO compared to that developed in this study was used to test the closure assumptions of the PDF models, because the data base could not provide all the necessary ingredients. Despite this simplification, it was possible to demonstrate that the current PDF models for NO overestimate significantly the NO production rate due to the fact that they neglect the correlations between the fluctuations in oxygen concentration and temperature. A single scalar PDF model for temperature that accounts for such correlations based on laminar flame considerations has been developed and showed excellent agreement with the values given by the DNS.

1. Introduction

This study is an investigation of the effects of chemistry and turbulence on nitric oxide formation in oxygen-natural gas flames. The choice of oxygen as the oxidizer is related to current interest in use of oxygen for high temperature combustion in

1 Air Liquide, Centre de Recherche Claude-Delorme, France
2 University of Southern California, Los Angeles, CA
3 Stanford University, Stanford, CA

industry. In terms of NO emissions, oxygen is advantageous compared to preheated air in high-temperature processes such as those encountered in the glass and steel making industry due to the low nitrogen content. However, molecular nitrogen still is present in certain amounts in the natural gas (0.5% for Algerian gas to 11% for Groningue gas) and in the oxygen stream. In the latter case, the nitrogen content depends on the production method: from virtually 0% for cryogenic oxygen to 5% for vacuum swing absorption. Other sources of nitrogen for oxygen-natural gas combustion include air leaks into the furnace. Despite the relatively low levels of NO emissions from oxy-combustion, ever more stringent emission standards require a better understanding of NO formation in oxy-flames.

The chemical mechanisms controlling NO formation are well known (Fenimore 1971, De Soete 1974, Miller & Bowman 1989, Drake & Blint 1991, Bozelli *et al.* 1993, Bowman 1992). Nitric oxide is formed from two sources: molecular nitrogen, N_2, and fuel-bound nitrogen. In the case of oxygen-natural gas flames, the only source is molecular nitrogen since natural gas, whatever its origin, does not contain nitrogen-bound species. In this case, the three main pathways for NO formation are the Zeldovich, prompt, and N_2O mechanisms, and the main pathway for NO destruction is the reburn mechanism. The Zeldovich mechanism is based on O-atom attack of N_2 through $O + N_2 = NO + N$, and is active both in the flame zone and the postflame zone. It is strongly dependent on temperature due to the high activation energy, $E_{Zeldovich}$, of the N_2-consuming step ($E_{Zeldovich} = 76.5\ kcal/mole$). A particular case of the Zeldovich mechanism is the equilibrium Zeldovich mechanism, where O-atoms are in partial equilibrium with molecular O_2. In this case, a global one-step reaction for NO formation can be derived with an overall activation energy, $E_{equilibrium} = 138\ kcal/mole$. The prompt mechanism is active only within the flame zone since it requires the presence of CH_x radicals for consumption of molecular nitrogen, mainly through $CH + N_2 = HCN + N$. Subsequent elementary reactions lead to the formation of NO. This mechanism is weakly dependent on temperature due to the low activation energy of the main N_2-consuming step ($E_{prompt} \cong 20$ kcal/mole). The N_2O mechanism is due to reaction of O-atoms with N_2 in a three-body reaction, i.e. $O + N_2 + M = N_2O + M$, with the subsequent reaction of N_20 to form mainly through $O + N_2O = NO + NO$. The reburn mechanism is responsible for consumption of NO within the flame zone to produce N_2, and it is controlled by CH, CH_2, and CH_3 radicals.

These various mechanisms are present in air flames and must be accounted for to predict accurately the level of nitric oxide emissions. The usual picture for NO production in air flames can be split in two parts: 1) production in the flame zone through a balance between the prompt, N_2O, and reburn mechanisms - in this zone, the Zeldovich mechanism can be neglected; 2) production of NO in the post-flame zone by the Zeldovich mechanism alone. The picture is different in oxygen flames since in this case, the destruction rate of N_2 is controlled by the Zeldovich mechanism, with a small contribution of the prompt mechanism (Samaniego *et al.* 1996). The main reason is that the higher temperatures of the oxygen flame tend to increase the destruction rates of N_2, and this acceleration is more pronounced

for the Zeldovich mechanism due to its higher activation energy. As a result, the Zeldovich mechanism becomes faster than the prompt NO mechanism in the flame zone of an oxygen flame, while it is slower than the prompt NO mechanism in the flame zone of an unpreheated air flame. However, it is not clear whether the NO production rates can be derived from the Zeldovich mechanism alone since reburn may be taking place as indicated by the high HCN concentration levels observed in the numerical study of Samaniego *et al.* (1996). Furthermore, it is necessary to clarify the role of non-equilibrium atomic oxygen since it is unclear whether the partial-equilibrium assumption holds (Samaniego *et al.* 1996).

The effect of turbulence on NO emissions in jet diffusion flames has been studied extensively (Peters & Donnerhack 1981, Turns & Myrh 1991, Chen & Kollman 1992, Driscoll *et al.* 1992). The turbulent mixing process results in temporal fluctuations in temperature and species composition which influence the NO formation rates. Since the relationships between NO formation rate, temperature, and species are highly non-linear, NO emissions cannot be predicted from mean temperature and species concentrations alone. Therefore, accurate predictions of NO formation rates require the knowledge of temperature and composition fluctuations. Modelers have derived PDF formulations that account for the effect of these fluctuations on the turbulent NO production rate (Janicka & Kollmann 1982, Pope & Correa 1986, Correa & Pope 1992). The closure of the turbulent source term for NO is made possible through the use of a joint PDF which, in the case of Zeldovich NO with the partial equilibrium assumption for atomic oxygen, can be expressed as:

$$\frac{d\overline{[NO]}}{dt} = \int k[O_2]^{1/2}[N_2]\exp(-E/RT)P([O_2],[N_2],T)\,d[O_2]\,d[N_2]\,dT \qquad (1)$$

where $P([O_2],[N_2],T)$ is a joint PDF of oxygen concentration, $[O_2]$, nitrogen concentration, $[N_2]$, and temperature, T. Usually, the nitrogen concentration is considered constant and $[N_2]$ is taken out of the PDF. Furthermore, in practice, $[O_2]$ and T are assumed to be independent variables and the joint PDF, P, can be expressed as the product of two single-variable PDF's, P_{O_2} and P_T, such as:

$$P([O_2],T) = P_{O_2}([O_2])P_T(T) \qquad (2)$$

In such a case, the turbulent NO production term becomes:

$$\frac{d\overline{[NO]}}{dt} = k\overline{[N_2]}\left(\int [O_2]^{1/2}P_{O_2}([O_2])d[O_2]\right)\left(\int \exp(-E/RT)P_T(T)dT\right) \qquad (3a)$$

In some cases, the same term is calculated from a single PDF by assuming that $[O_2]$ fluctuations can be neglected:

$$\frac{d\overline{[NO]}}{dt} = k\overline{[N_2][O_2]}^{1/2}\left(\int \exp(-E/RT)P_T(T)dT\right) \qquad (3b)$$

In both cases, this final assumption has a limited domain of validity since it presumes that the oxygen concentration fluctuations are not correlated with the temperature fluctuations. This may be valid in the post-flame zone where the combustion process is completed, but it is highly questionable in the flame zone where the temperature and oxygen concentration levels are obviously correlated. Since the amount of NO produced in the flame zone of oxygen flames can be very significant, it is expected that such PDF modeling approaches are inapplicable.

The goals of this study are to derive a simple chemical model for NO formation in oxygen diffusion flames and to propose a model for the closure of the turbulent NO production term based on a PDF approach. For this purpose, two complementary numerical approaches are used, one addressing the effects of chemistry, and another addressing the effect of turbulence.

2. Effects of chemistry

2.1 Numerical approach

Concerning chemistry, NO formation mechanisms are investigated using the counterflow flame problem. The counterflow configuration is often used to address chemistry-turbulence interactions with detailed chemistry, and it is well known that the strain-rate modifies the chemical pathways through reduced flame temperature reduction and residence times (Hahn and Wendt 1981, Haworth *et al.* 1988, Drake and Blint 1989, Chelliah *et al.* 1990, Mauss *et al.* 1990, Vranos *et al.* 1992, Takeno *et al.* 1993, Egolfopoulos 1994a, 1994b, Nishioka *et al.* 1994, Samaniego *et al.* 1995, Egolfopoulos & Campbell 1996). In such a geometry, the flow field is that of a strained flame where a jet of oxidizer impinges upon a jet of fuel. The oxidizer is a mixture of oxygen and nitrogen. Various mixtures are used: 100% O_2 and 0% N_2; 95% O_2 and 5% N_2; 21% O_2 and 79% N_2. The fuel is a mixture of methane and nitrogen. Two different mixtures are used: 100% CH_4 and 0% N_2; 95% CH_4 and 5% N_2.

The numerical simulation is conducted by solving the steady and unsteady equations of mass, momentum, energy, and species concentrations along the streamline. Details on the set of equations and numerical method can be found in Egolfopoulos (1994a and 1994b), and in Egolfopoulos & Campbell (1996). The chemical scheme that is used for combustion of methane is the latest GRI 2.11 mechanism, which accounts for 49 species and 277 reactions. Calculations are performed without radiative losses as it has been demonstrated that radiative losses from CO_2, H_2O, CO, and CH_4 play a negligible role in counterflow oxygen flames (Samaniego *et al.* 1996).

2.2 Results

The objective of this study is to check whether the Zeldovich mechanism alone is capable of predicting with sufficient precision the rate of formation of NO in an oxygen flame. In order to do so, two sets of calculations have been carried out, one with the full mechanism which includes all NO formation routes, and one with the three reactions of the Zeldovich mechanism, namely:

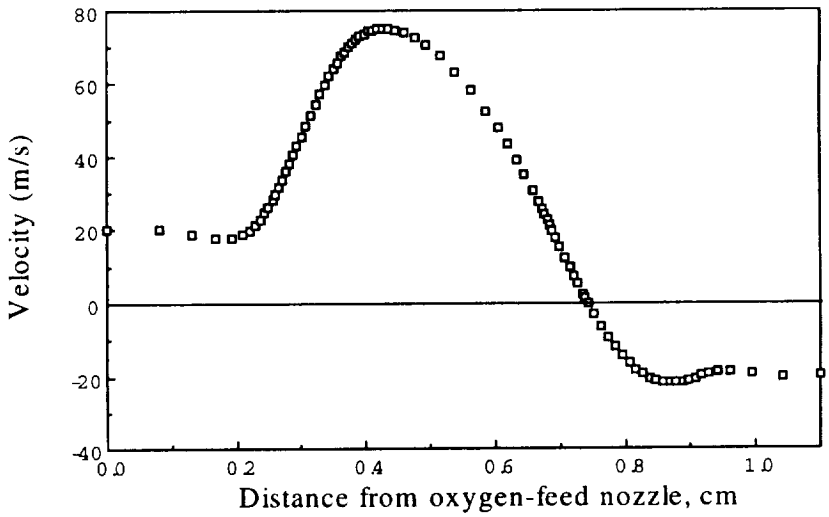

FIGURE 1. Computed velocity profile along the stagnation streamline of a counterflow O_2/CH_4 flame for a strain-rate of 25 s^{-1}.

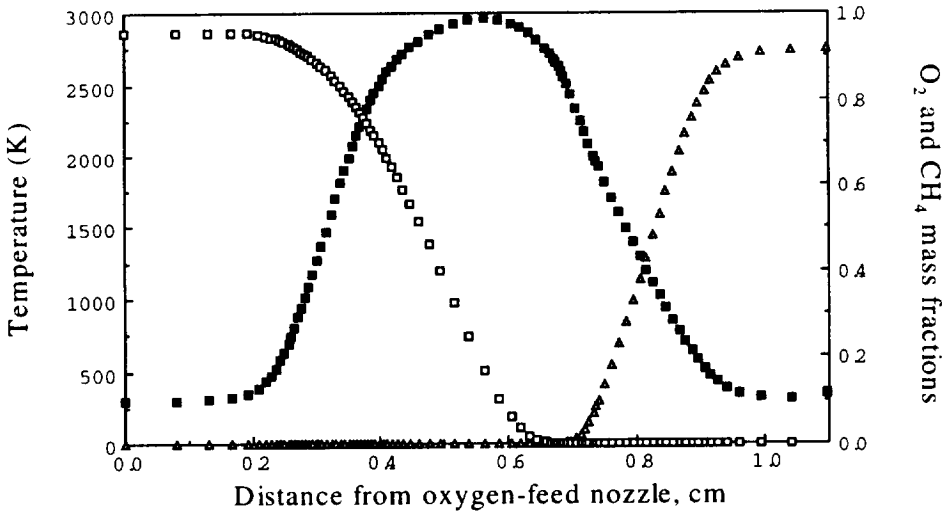

FIGURE 2. Computed profiles of temperature (■), oxygen mass fraction (□) and methane mass fraction (△) in a counterflow O_2/CH_4 flame for a strain-rate of 25 s^{-1}.

$$O + N_2 = NO + N \qquad (R1)$$

$$N + O_2 = NO + O \qquad (R2)$$

$$N + OH = NO + H \qquad (R3)$$

For both mechanisms, a series of about 400 steady strained flames is calculated for strain-rates varying from 10 to 1000 s^{-1}. The strain-rate is defined as the maximum velocity gradient in the oxidant stream. Figures 1 and 2 depict the flame structure for a strain-rate of 25 s^{-1}, which is typical of all the strain-rates computed in this study. This result is obtained with the full GRI 2.11 mechanism, and it is almost identical for the Zeldovich calculations since the NO chemistry does not significantly impact the fuel chemistry. The horizontal axis is the co-ordinate along the stagnation streamline, with oxidant being fed at $x = 0$ cm and fuel being fed at $x = 1.05$ cm. The feed velocities in this case are $V = 20$ cm/s for both streams. The velocity profile exhibits a stagnation point at $x = 0.74$ cm (Fig. 1). The velocity decreases from the oxygen nozzle feed, then increases due to thermal expansion and decreases again until crossing the stagnation point. The velocity profile has a similar behavior on the fuel side, and asymmetries are due to the different molecular weights of O_2 and CH_4 and to chemical effects. Figure 2 depicts the profiles of mass fractions of O_2, CH_4, and temperature. The maximum temperature is reached at $x = 0.56$ cm which corresponds to the flame zone. The consumption of oxygen and methane are almost complete at $x = 0.65$ cm, a location slightly on the fuel side relative to the maximum temperature. This can be attributed to the fact that some recombination reactions, which are exothermic, occur on the oxygen side. Figure 3 depicts the profile of NO mass fraction, Y_{NO}, in the case of the full and Zeldovich mechanisms, and in this case both mechanisms give similar maximum values but slightly different profiles in the fuel side.

To allow comparison with well known results, a series of strained unpreheated air flames also has been calculated. Figure 4 depicts the maximum NO mass fractions, $Y_{NO,max}$, as a function of strain-rate for the oxygen and air flames, and for the Zeldovich and full mechanisms. In all cases, $Y_{NO,max}$ decreases with increasing strain-rate, and this can be attributed to reduced residence times. In the case of the oxygen flame, $Y_{NO,max}$ is well predicted by the Zeldovich mechanism alone. In contrast, in the case of the air flame, $Y_{NO,max}$ is underpredicted by the Zeldovich mechanism by one to three orders of magnitude. The difference in behavior between the air and oxygen flames can be explained on the basis of the flame temperature as indicated in Samaniego *et al.* (1996). Oxygen flames are much hotter than air flames and, as a consequence, the Zeldovich mechanism, which is highly sensitive to temperature, is predominant over the prompt mechanism; in contrast, air flames are not as hot and the prompt mechanism is predominant over the Zeldovich mechanism at all strain-rates (Drake & Blint 1989, Nishioka *et al.* 1994).

A further comparison between full and Zeldovich mechanisms for the oxygen flame is performed by plotting the integral of the N_2 consumption rate, $\int(-d[N_2]/dt)dx$, as a function of strain-rate for both calculations. The reason for looking at this

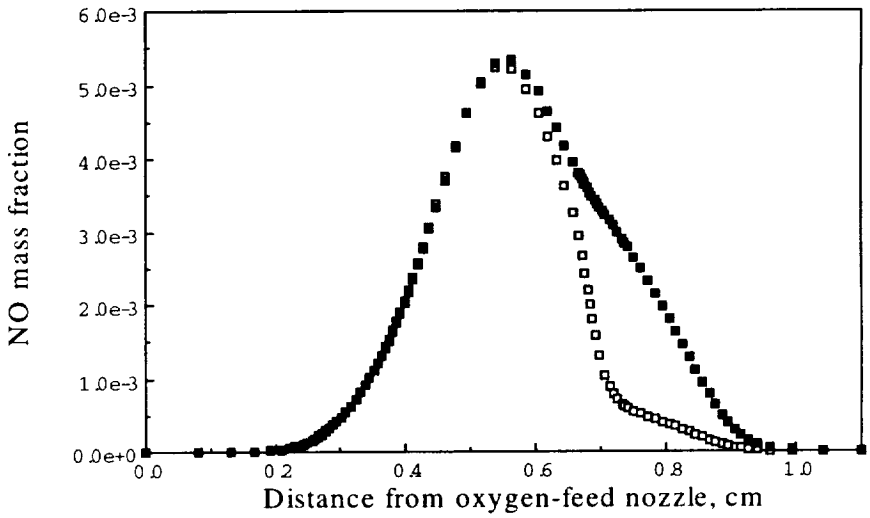

FIGURE 3. Computed profiles of NO mass fraction in a counterflow O_2/CH_4 flame with 5% N_2 addition in both streams for a strain-rate of 25 s^{-1}. Filled symbols: full GRI 2.11 mechanism. Open symbols: Zeldovich mechanism alone.

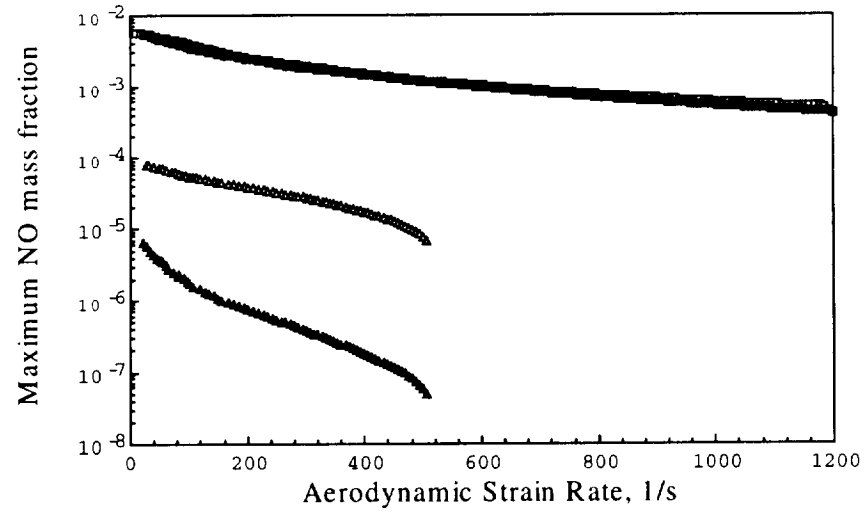

FIGURE 4. Effect of strain-rate on maximum NO mass fraction. □: Full GRI 2.11 mechanism for a O_2/CH_4 counterflow diffusion flame with 5% N_2 addition in both streams. ■: Zeldovich mechanism alone for a O_2/CH_4 counterflow diffusion flame with 5% N_2 addition in both streams. △: Full GRI 2.11 mechanism for an unpreheated Air/CH_4 counterflow diffusion flame. ▲: Zeldovich mechanism alone for an unpreheated Air/CH_4 counterflow diffusion flame.

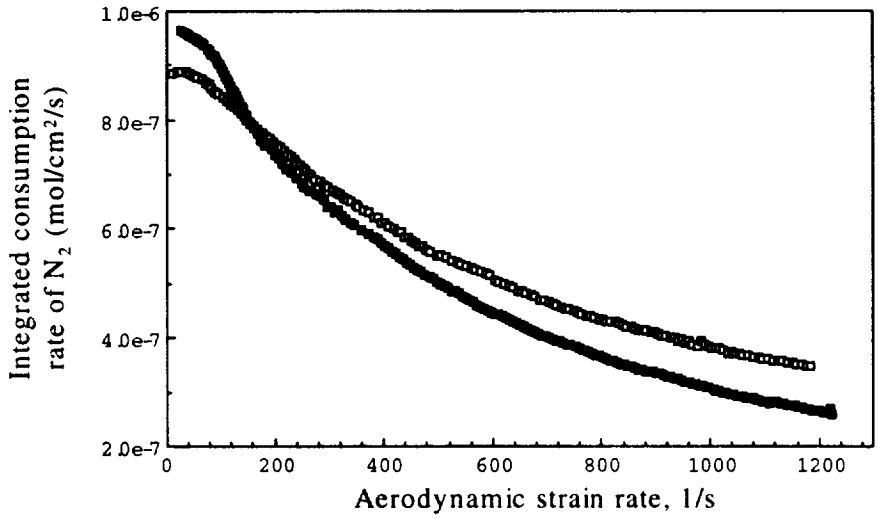

FIGURE 5. Effect of strain-rate on integrated consumption rate of N_2. □: Full GRI 2.11 mechanism for a O_2/CH_4 counterflow diffusion flame with 5% N_2 addition in both streams. ■: Zeldovich mechanism alone for a O_2/CH_4 counterflow diffusion flame with 5% N_2 addition in both streams.

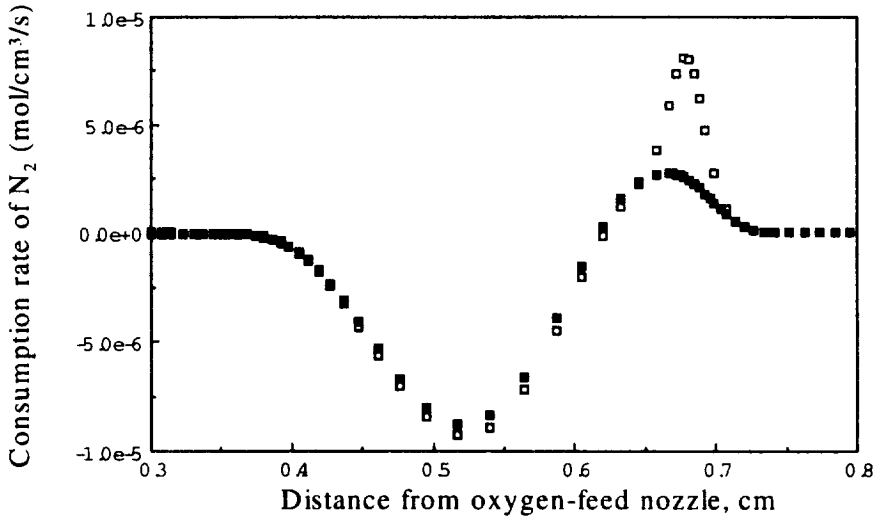

FIGURE 6. Profile of N_2 consumption rate in a strained O_2/CH_4 counterflow diffusion flame with 5% N_2 addition in both streams for a strain-rate of 25 s^{-1}. □: Full GRI 2.11 mechanism. ■: Zeldovich mechanism alone.

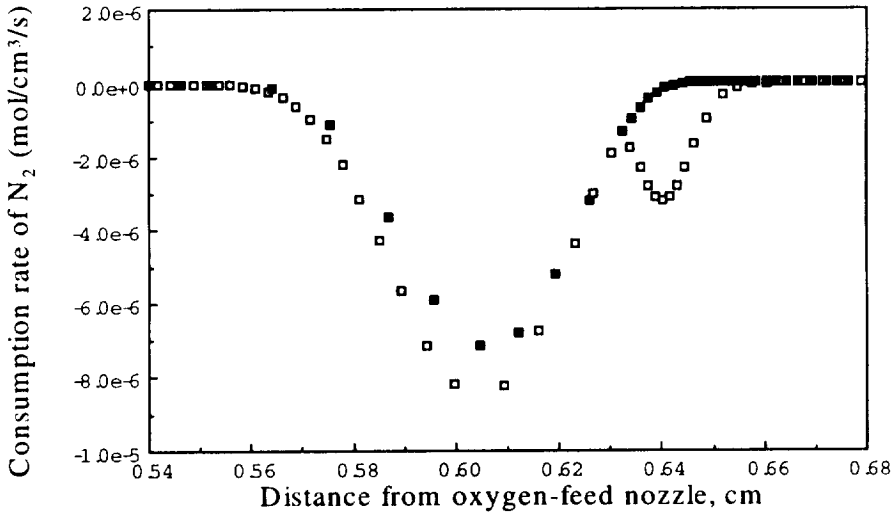

FIGURE 7. Profile of N_2 consumption rate in a strained O_2/CH_4 counterflow diffusion flame with 5% N_2 addition in both streams for a strain-rate of 1065 s^{-1}. □: Full GRI 2.11 mechanism. ■: Zeldovich mechanism alone.

quantity rather than the flux of NO is that reburn, i.e. production of N_2 from NO and other nitrogen-containing species, can be clearly identified. Figure 5 depicts that, in both cases, the consumption rate of N_2 is positive and decreases with strain-rate. Furthermore, the Zeldovich approach shows two weaknesses: 1) at low strain-rates, it overpredicts the consumption of N_2, and 2) at high strain-rates, it underpredicts it. Overprediction of N_2 consumption at low strain-rates is evidence that reburn through the hydrocarbon chemistry is active in these cases, and underprediction at high strain-rates indicates that N_2 consumption through the prompt mechanism is significant.

The discrepancies between the full and Zeldovich mechanisms may be explained by analyzing the profile of $d[N_2]/dt$ at low and high strain-rates. Figure 6 depicts the profiles of $d[N_2]/dt$ for both mechanisms and the profiles of temperature, oxygen mass fraction, and methane mass fraction for a strain-rate of 25 s^{-1}. For both mechanisms, $d[N_2]/dt$ is negative on the oxygen side and positive on the fuel side. On the oxygen side, N_2 is consumed to produce NO and other nitrogen-containing species and the two mechanisms give similar results. This indicates that N_2 consumption is mainly due to the Zeldovich mechanism via the reaction $O + N_2 \rightarrow NO + N$ and that the prompt and reburn mechanisms are not active. On the fuel side, N_2 is produced, which is evidence of reburn, and there is a significant discrepancy between the full and Zeldovich mechanisms. In this case, the Zeldovich pathway predicts some reburn through the reverse reaction ($N + NO \rightarrow O + N_2$) but misses the reburn through hydrocarbon chemistry which is accounted for by the full GRI 2.11 reaction mechanism. The picture is different at higher strain-rates. Figure 7 depicts the profiles of $d[N_2]/dt$ for both mechanisms and the profiles of temperature, oxygen

mass fraction and methane mass fraction for a strain-rate of 1065 s^{-1}. In this case, $d[N_2]/dt$ is always negative everywhere in the flame for both the Zeldovich and full mechanisms, indicating that there is no reburn. However, the full GRI 2.11 scheme predicts higher consumption rates of N_2 everywhere in the flame zone both on the oxygen side and in the fuel side. On the oxygen side, most of the N_2 is consumed via the Zeldovich mechanism, but additional reactions are also taking place. On the fuel side, the full mechanism exhibits a "bump" that is missed by the Zeldovich mechanism and which is due to the "prompt" reaction, $CH + N_2 \rightarrow N + HCN$.

Therefore, the following picture can be drawn for oxygen flames: 1) the amount of N_2 consumption and, consequently, NO production decreases by about 50% for strain-rates varying between 10 and 1000 s^{-1}; 2) in this range of strain-rates, the Zeldovich mechanism predicts N_2 consumption within ± 25% compared to the full GRI mechanism; 3) at low strain-rates, the Zeldovich mechanism overpredicts N_2 consumption by about 15% because it does not account for reburn through the hydrocarbon chemistry; 4) at high strain-rates, the Zeldovich mechanism underpredicts the N_2 consumption by about 25% because it does not account for N_2 consumption through the prompt mechanism.

2.3 An overall one-step model for N_2 consumption

The next step consists in deriving an overall one-step reaction mechanism for N_2 consumption based on the Zeldovich mechanism alone. The proposed model (model 1) includes reburn and considers the following reactions:

$$NO + N = N_2 + O \qquad (R1)$$

$$N + O_2 = O + NO \qquad (R2)$$

$$N + OH = H + NO \qquad (R3)$$

$$H + O_2 = OH + O \qquad (R4)$$

$$H + OH + M = H_2O + M \qquad (R5)$$

$$O + O + M = O_2 + M \qquad (R6)$$

The model is based on the following: 1) reaction 2 plays a negligible role (its net reaction rate is 1 to 2 orders of magnitude less than those of reactions 1 and 3); 2) atomic nitrogen is in steady-state ($d[N]/dt = 0$); 3) reactions 4 to 6 are assumed in partial equilibrium. After some algebra and considering N-atom conservation, one finds:

$$\frac{d[NO]}{dt} = -2\frac{d[N_2]}{dt} = 2\frac{k_1^+ k_3^- [H][NO]^2 - k_1^- k_3^+ [N_2][OH][O]}{k_1^+ [NO] + k_3^+ [OH]} \qquad (4)$$

with

$$[H] = \left[\frac{[H_2O][O]}{K_4 K_5 [O_2]}\right]^{1/2} \qquad (5)$$

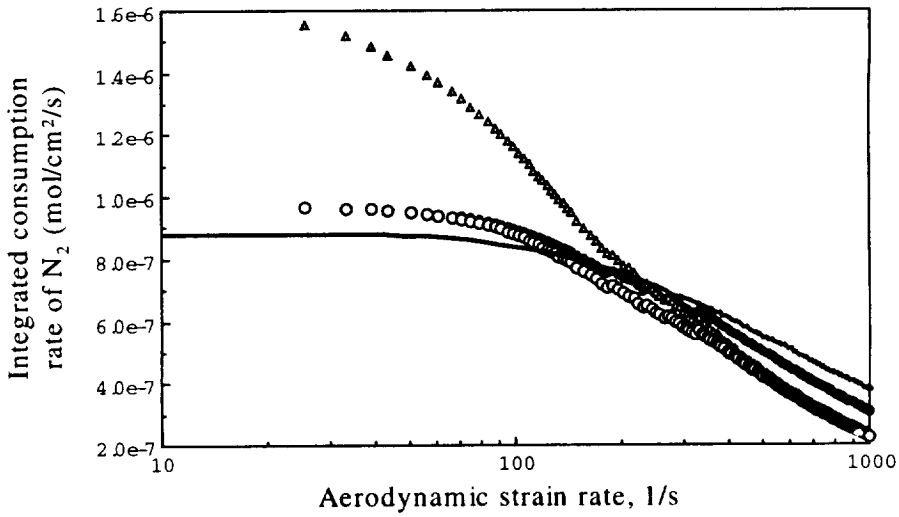

FIGURE 8. Effect of strain-rate on integrated consumption rate of N_2 in a O_2/CH_4 counterflow diffusion flame with 5% N_2 addition in both streams. Solid line: Full GRI 2.11 mechanism. • : Zeldovich mechanism alone. Δ: model with no reburn. ▲: model with reburn.

$$[OH] = \left[\frac{K_4[H_2O][O_2]}{K_5[O]}\right]^{1/2} \tag{6}$$

$$[O] = \left[\frac{[O_2]}{K_6}\right]^{1/2} \tag{7}$$

where bracketed quantities refer to concentrations, and where k is the specific reaction rate, K is the equilibrium constant, subscripts refer to reaction numbers, superscript '+' refers to forward rate of reaction, and superscript '-' refers to backward rate of reaction.

An alternative model (model 2) with no reburn effects and with the partial equilibrium assumption for atomic oxygen can be derived by assuming $k_1^+ = 0$. One obtains:

$$\left.\frac{d[NO]}{dt}\right|_{\text{no reburn}} = -2\left.\frac{d[N_2]}{dt}\right|_{\text{no reburn}} = 2\frac{k_1^-}{K_6^{1/2}}[O_2]^{1/2}[N_2] \tag{8}$$

These global one-step models are compared with the full GRI 2.11 and the Zeldovich mechanisms by focusing on the evolution of the spatially-integrated N_2 consumption rate with strain-rate (Fig. 8). This figure also depicts the values of $\int(-d[N_2]/dt)dx$ of the full GRI 2.11 and Zeldovich mechanisms. As in Fig. 5, all models lead to a decrease of the integrated consumption rate of N_2 with strain-rate. Model 1 has a behavior similar to the Zeldovich mechanism except that at strain-rates greater than 200 s^{-1} it underpredicts N_2 consumption. This is due

to the fact that for the higher strain-rates the partial equilibrium assumption for atomic oxygen fails. Compared to the full GRI 2.11 scheme, model 1 overpredicts N_2 consumption at low strain-rates by about 15% due to the fact that it does not account for reburn through the hydrocarbon chemistry. At high strain-rates, it underpredicts N_2 consumption by about 50% due to the fact that it does not account for the prompt mechanism and for non-equilibrium effects of atomic oxygen. Model 2 overpredicts significantly N_2 consumption at low strain-rates and behaves like model 1 at high strain-rates. The overprediction of N_2 consumption is due to the fact that no reburn mechanism is included, neither that of the Zeldovich mechanism alone, nor that of the full GRI 2.11 scheme. This shows that inclusion of the reverse step, $N + NO \rightarrow N_2 + O$, is essential in getting correct estimates of N_2 consumption at low strain-rates.

3. Effect of turbulence

3.1 Numerical approach

Concerning turbulence, the closure method is investigated by post-processing the 3D data base of a turbulent diffusion flame developed by Vervisch (1992). This data base was the result of a direct numerical simulation of a turbulent non-premixed flame in decaying turbulence. The flow field was resolved accurately by solving the full Navier-Stokes equations. The flame was modeled by a one-step irreversible reaction, $O + F \rightarrow P$, where O is the oxidizer, F is the fuel, and P is the product, and the reaction rate follows an Arrhenius formulation:

$$\dot{w} = k\rho Y_O \rho Y_F \exp(-E/RT) \tag{9}$$

where $\dot{w}$ is the reaction rate, k is the pre-exponential factor, ρ is the density, Y_O is the oxidizer concentration, Y_F is the fuel concentration, E is the activation energy, R is the gas constant, and T is the temperature. The formalism that was used was that of Williams (1985): the quantities were non-dimensionalized in such a way that the heat of reaction was expressed in terms of a temperature jump, $\alpha = (T_b - T_u)/T_b$ and the activation energy was expressed in terms of a Zeldovich number, $\beta = E(T_b - T_u)/RT_b{}^2$. The values of these parameters are: $\alpha = 0.8$ and $\beta = 8$. The pre-exponential factor was selected such that the initial global Damköhler number was equal to one. This number is defined in Chen *et al.* (1992) as:

$$Da = \frac{l_t}{u_0}\left[\frac{1}{\delta_{fl}}\int_{\delta_{fl}} \dot{w}dx\right] \tag{10}$$

where l_t is the integral scale of turbulence, u_0 is the rms velocity, and δ_{fl} is the flame thickness. The Damköhler number expresses the ratio between the initial eddy turnover time and a characteristic chemical time. Furthermore, the molecular weights of the fuel and the oxidizer were taken to be equal.

At time $t = 0$, the flow field was initialized with a given spectrum for turbulence and with a planar laminar diffusion flame located at the center of the computational

domain. The calculations were carried out on a 129 × 65 × 65 grid. The resulting data base is composed of a series of eight different time intervals: they correspond to times 0, 2.1, 4.4, 6.8, 9.2, 10.0, 14.7, 17.2, where time is non-dimensionalized by the acoustic time, $t_a = L/c$ (c is the speed of sound in the fresh reactants and L is a reference length).

The approach for testing various modeling formulations consists of computing at each time-step the volume-average of $d[N_2]/dt$ and comparing this value with that given by the various closure models. To compute $d[N_2]/dt$, a chemical model is needed, and we use model 2 in this section. The reason for not using model 1 is that it is necessary to have the NO concentration for this model. However, the data base does not provide this information, but provides the oxidizer mass fraction and the temperature field, and, therefore, only model 2 can be used. Consequently, reburn is not accounted for. Since the objective is to assess closure formulations, it is expected that model 2 is sufficient. In this case, the consumption rate of NO is expressed from Eq. 8 as follows:

$$\frac{d[NO]}{dt} \sim \sqrt{\frac{Y_O}{T}} \frac{1}{T} \exp(-T_a/T) \tag{11}$$

where Y_O/T is assumed to be proportional to $[O_2]$, $1/T$ is assumed to be proportional to $[N_2]$, and T_a is the activation temperature. In this data base, T is non-dimensional and varies between 2.5 and 12.5; therefore, T_a is non-dimensional and is set equal to:

$$T_a = \frac{E_{Equilibrium}(cal/mol)}{R(cal/mol/K)} \times \frac{12.5}{T_b(K)} \tag{12}$$

Here, we take $T_b = 3000\ K$ in order to reproduce the temperature sensitivity of N_2 consumption occurring in an oxygen-methane flame, and this leads to $T_a = 287.5$. Consequently, the exact turbulent production of NO in the direct numerical simulation is taken to be:

$$\frac{d[NO]}{dt}|_{\text{exact}} = \frac{1}{N_x N_y N_z} \Sigma_{Nx,Ny,Nz} \frac{\sqrt{Y_O}}{T^{3/2}} \exp(-T_a/T) \tag{13}$$

where N_x, N_y and N_z are the number of points in directions x, y and z, respectively.

3.2 Results

The PDF closure models of Eq. 3a, referred to as JPDF for joint PDF, and Eq. 3b, referred to as SPDF for single PDF, are assessed by comparing their predictions with the actual NO production rates as estimated from Eq. 13. The predictions by JPDF and SPDF are computed as follows:

$$\left.\frac{d[NO]}{dt}\right|_{\text{JPDF}} =$$

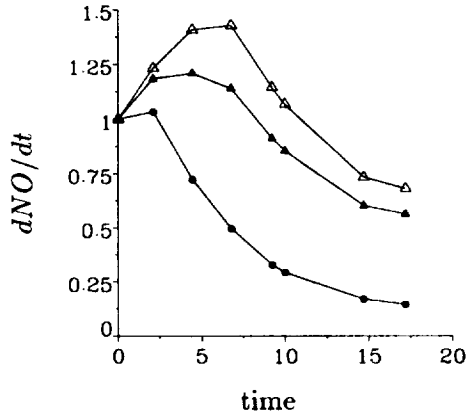

FIGURE 9. Time-evolution of turbulent NO production term. The terms are non-dimensionalized by the exact value at $t = 0$. • : Exact term. ▲: Joint PDF. △: Single scalar PDF.

$$\frac{1}{Nx}\Sigma_{Nx}\left(\frac{1}{N_yN_z}\Sigma_{N_y,N_z}\frac{1}{T}\right)\left(\frac{1}{N_yN_z}\Sigma_{N_y,N_z}\sqrt{\frac{Y_O}{T}}\right)\left(\frac{1}{N_yN_z}\Sigma_{N_y,N_z}\exp(T_a/T)\right) \tag{14a}$$

$$\left.\frac{d[NO]}{dt}\right|_{\text{SPDF}} =$$

$$\frac{1}{Nx}\Sigma_{Nx}\left(\frac{1}{N_yN_z}\Sigma_{N_y,N_z}\frac{1}{T}\right)\left(\sqrt{\frac{1}{N_yN_z}\Sigma_{N_y,N_z}\frac{Y_O}{T}}\right)\left(\frac{1}{N_yN_z}\Sigma_{N_y,N_z}\exp(T_a/T)\right) \tag{14b}$$

Figure 9 shows a comparison between the predictions of JPDF, SPDF, and the exact $d[NO]/dt$. In all cases, the production rate of NO starts increasing and then decreases at later times. This can be explained as follows: at initial times, the flame surface is wrinkled by turbulence, leading to an increase of flame surface area and, therefore, to an increase in NO production; at later times, the flame is strained by the turbulent flow field and is locally quenched, as can be seen in Chen *et al.* (1992), thereby reducing the rate of production of NO. The JPDF and SPDF models overestimate significantly the amount of NO production rates, with JPDF being slightly better than SPDF. The reason for this overestimation is that $[O_2]$ and T are assumed to be uncorrelated. This can be seen as follows (for simplicity, we consider $[N_2]$ as constant):

$$\frac{d\overline{[NO]}}{dt} \sim \overline{[O_2]^{1/2}\exp(T_a/T)} = ([O_2]^{1/2})^*\overline{\exp(-T_a/T)} \tag{15}$$

where $([O_2]^{1/2})^*$ is a weighted average of $[O_2]^{1/2}$ with:

$$([O_2]^{1/2})^* = \int_V [O_2]^{1/2}\left(\frac{\exp(-T_a/T)}{\int_V \exp(-T_a/T)dV}\right)dV \tag{16}$$

where V is the volume on which is conducted the averaging procedure, here, the computational domain. Equation 16 is a weighted average which is strongly biased towards the high temperatures and, therefore, strongly biased to low values of $[O_2]$, due to chemical reaction and dilatation. Consequently, we obtain:

$$([O_2]^{1/2})^* < \overline{[O_2]^{1/2}} \tag{17}$$

Furthermore, we have:

$$\overline{[O_2]^{1/2}} < \overline{[O_2]}^{1/2} \tag{18}$$

By combining Eq. 15, 17, and 18 and assuming that $[N_2]$ inhomogeneities do not modify the relationships, one finds:

$$\int_V [N_2][O_2]^{1/2} \exp(-T_a/T)dV < \overline{[N_2]}\left(\int_V [O_2]^{1/2}dV\right)\left(\int_V \exp(-T_a/T)dV\right)$$

$$< \overline{[N_2]}\ \overline{[O_2]}^{1/2} \int_V \exp(-T_a/T)dV \tag{19}$$

Therefore, not accounting for the correlation between $[O_2]$ and T leads necessarily to an overestimation of the turbulent production term of NO. In addition, the error is dependent on the averaging volume as is apparent in Eq. 16. In the case of Fig. 9, the averaging volumes over which are computed mean quantities are yz planes as indicated in Eq. 14a and 14b, and this corresponds to a case that minimizes the error. Additional computations have been carried where a single averaging volume corresponding to the whole computational domain has been used, and the corresponding estimates of $d\overline{[NO]}/dt$ by the SPDF and JPDF models are 20 times higher.

3.3 A model based on laminar flame structure

To improve the predictive capabilities of PDF formulations for NO formation, a correlation between $[O_2]$ and T is sought assuming a laminar flame structure. The goal is to express $[O_2]$ as a function of temperature. Figure 10 shows the correlation between Y_O and the reduced temperature θ at time $t = 0$ in the data base, where θ is defined by:

$$\theta = \frac{T - T_u}{T_b - T_u} \tag{20}$$

The relationship has two branches, one with high values of Y_O corresponding to the oxidizer side, and one with low values of Y_O corresponding to the fuel side. Matching the oxidizer branch leads to the following fit:

$$Y_O = 1. - 0.9 \times \theta \tag{21}$$

and the fuel branch is fit by:

$$Y_O = 0.05 \times \theta \tag{22}$$

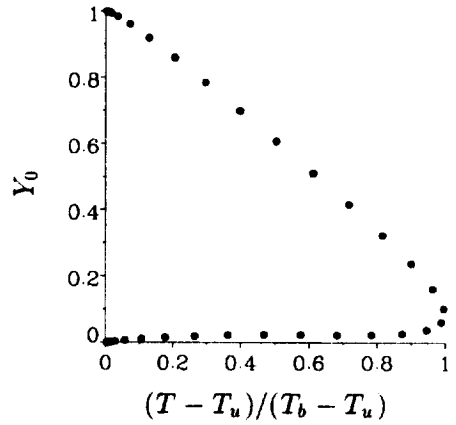

FIGURE 10. Relationship between θ and Y_O across the planar laminar diffusion flame at time $t = 0$ in the data base.

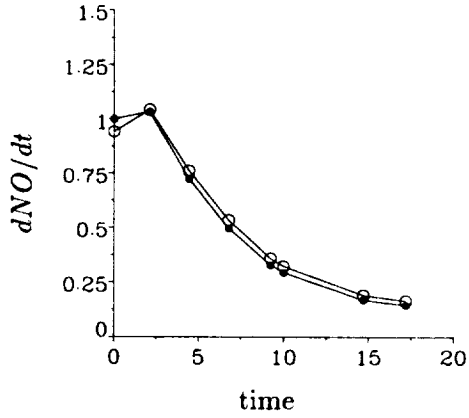

FIGURE 11. Time-evolution of turbulent NO production term. The terms are non-dimensionalized by the exact value at $t = 0$. • : Exact term. o : proposed single scalar PDF model.

Combining Eq. 13, 21, and 22 leads to the following alternate single PDF model:

$$\left.\frac{d[NO]}{dt}\right|_{\text{model}} = \frac{1}{N_x N_y N_z} \Sigma_{Nx,Ny,Nz} \frac{1}{2} \left(\frac{\sqrt{1-0.9\theta}}{T^{3/2}} + \frac{\sqrt{0.05\theta}}{T^{3/2}} \right) \exp(-T_a/T) \quad (23)$$

Figure 11 shows the evolution of the turbulent production term of NO for the new single PDF model. The agreement is very good and the predictions of this new model are insensitive to the choice of the averaging volume.

This test shows that this new model is promising and can be applied in practical codes that use single PDF formulations for NO production. In the case of an oxygen-natural gas flame, reburn should be accounted for and concentrations of O_2, H_2O, and NO should be included. Therefore, correlations between $[O_2]$ and

T, $[H_2O]$ and T,and $[NO]$ and T should be derived from, for example, a library of laminar strained flames.

In practice, this PDF model would be able to predict the amount of NO produced in the flame zone; however, it would not be appropriate in the post-flame zone since $[O_2]$ and T are no longer correlated. Therefore, two models should be used, one for the reaction zone, similar to that developed in this paper, and one for the post-flame zone of the kind of the SPDF or JPDF models.

4. Conclusion

The effects of chemistry and turbulence on the rate of production of nitric oxide in oxygen-natural gas diffusion flames has been investigated.

It has been shown that, due to the high temperatures encountered in these flames, the Zeldovich mechanism is dominant and accounts for more than 75% of the rate of production of NO over a large range of strain-rates. The limitations of predictions based on the Zeldovich mechanism alone have been identified: at low strain-rates, it overpredicts N_2 consumption, which is the source of NO, due to the fact that it does not account for reburn, and at high strain-rates it underpredicts N_2 consumption due to the fact that it does not account for the prompt mechanism. Despite these shortcomings, the Zeldovich mechanism is satisfactory for predicting NO formation rates within 25% and an overall one-step mechanism that accounts for reburn and which assumes partial equilibrium of atomic oxygen with O_2 has been developed. This simple model gives the same results as the Zeldovich mechanism at low strain-rates but leads to further underprediction of N_2 consumption due to the fact that it cannot reproduce non-equilibrium effects.

The effect of turbulence is to generate fluctuations of temperature and species concentrations as well as straining effects. It has been shown by postprocessing the 3D DNS data base of Vervisch (1992) that usual closure models based on single scalar PDF's or joint PDF's lead to significant overpredictions of NO formation rates. The main reason is that these models do not account for the intrinsic correlation between oxygen concentration and temperature in the reaction zone of a diffusion flame. A new single scalar PDF model incorporating such a correlation has been developed. The model assumes that the relationship between oxygen and temperature is that of a laminar diffusion flame. The predictions of this model are in excellent agreement with the results from the DNS, and it is expected that it can be implemented in practical codes that use single scalar PDF's for NO formation.

Acknowledgments

The first author would like to thank Prof. P. Moin for giving the opportunity to participate to this summer program. He would also like to thank Greg Ruetsch and Nigel Smith for their help. The second author would like to express his gratitude to Air Liquide and CTR for their partial financial support.

REFERENCES

BOWMAN, C. T. 1992 Control of combustion-generated nitrogen oxide emissions:

Technology driven by regulation. *24th Symposium (Int'l.) on Combustion*, The Combustion Institute, Pittsburgh, 859-878.

BOWMAN, C. T., HANSON, R. K., DAVIDSON, D. I., GARDINER, W. C., LISSIANSKI, V., FRENKLACH, M., GOLDENBERG, M., SMITH, G. P., GOLDEN, G. M. AND SERAISKAR, R. V. Optimized Kinetics for Natural Gas Combustion, NO_x Production and Reburning (GRI Mech 2.11) Poster 047, *26th* Int. Symposium on Combustion.

BOZELLI, J. W., KARIM, M. H. U. & DEAN, A. M. 1993 Reactions of CH2 and CH with N2 and CH with NO. In *Turbulence and Molecular Processes in Combustion*, Elsevier Science Publishers B. V., Amsterdam, 101.

CHELLIAH, H. K., LAW, C. K., UEDA, T., SMOOKE, M. D. & WILLIAMS, F. A. 1990 An experimental and theoretical investigation of the dilution, pressure and flow-field effects on the extinction condition of methane-air-nitrogen diffusion flames. *23rd Symposium (Int'l.) on Combustion.* The Combustion Institute, Pittsburgh, 503-511.

CHEN, J. H., MAHALINGAM, S., PURI, I. K. & VERVISCH, L. 1992 Effect of finite-rate chemistry and unequal Schmidt numbers on turbulent non-premixed flames modeled with single-step chemistry. *Proceedings of the 1992 Summer Program*, Center for Turbulence Research, Stanford Univ./NASA Ames, 367-387.

CHEN, J.-Y. & KOLLMANN, W. 1992 PDF modeling and analysis of thermal NO formation in turbulent nonpremixed hydrogen-air jet flames. *Combust. Flame* **88**, 37-49.

CORREA, S. M.& POPE, S. B. 1992 Comparison of a Monte Carlo PDF/Finite-Volume Mean Flow Model with Bluff-Body Raman Data. *Twenty-Fourth Symposium (Int'l.) on Combustion*,The Combustion Institute, 279-285.

DE SOETE, G. G. 1974 Overall reaction rates of NO and N2 formation from fuel dilution. *15th Symposium (Int'l.) on Combustion.* The Combustion Institute, Pittsburgh, 1093-1102.

DRAKE, M. C. & BLINT 1989 Thermal NOx in stretched laminar opposed-flow diffusion flames with CO/H2/N2 fuel. *Combust. Flame* **76**, 151-167.

DRAKE, M. C. & BLINT 1991 Relative importance of nitric oxide formation mechanisms in laminar opposed-flow diffusion flames. *Combust. Flame* **83**, 287-338.

DRISCOLL, J. F., CHEN, R.-H. & YOON, Y. 1992 Nitric oxide levels of turbulent jet diffusion flames: Effects of residence time and Damköhler number. *Combust. Flame* **88**, 37-49.

EGOLFOPOULOS, F. N. 1994a Dynamics and Structure of Unsteady, Strained, Laminar, Premixed Flames. *25th Symposium (Int'l.) on Combustion.* The Combustion Institute, Pittsburgh, 1365-1374.

EGOLFOPOULOS, F. N. 1994b Geometric and Radiation Effects on Steady and Unsteady Strained Laminar Flames. *25th Symposium (Int'l.) on Combustion.* The Combustion Institute, Pittsburgh, 1375-1381.

EGOLFOPOULOS, F. N. & CAMPBELL, C. S. 1996 Unsteady, Counterflowing, Strained Diffusion Flames: Frequency Response and Scaling. *J. of Fluid Mech.* **318**, 1-29.

FENIMORE, C. P. 1971 Formation of nitric oxide in premixed hydrocarbon flames. *13th Symposium (Int'l.) on Combustion.* The Combustion Institute, Pittsburgh, 373-380.

HAHN, W. A. & WENDT, J. O. L. 1981 NOx formation in flat, laminar, opposed jet methane diffusion flames. *18th Symposium (Int'l.) on Combustion.* The Combustion Institute, Pittsburgh, 121-131.

HAWORTH, D. C., DRAKE, M. C., POPE, S. B. & BLINT, R. J. 1988 The importance of time-dependent flame structures in stretched laminar flamelet models for turbulent jet diffusion flames. *22nd Symposium (Int'l.) on Combustion.* The Combustion Institute, Pittsburgh, 589-597.

JANICKA, J. & KOLLMANN, W. 1982 The Calculation of Mean Radical Concentrations in Turbulent Diffusion Flames. *Combust. Flame.* **44,** 319-336.

MAUSS, F., KELLER, D. & PETERS, N. 1990 A lagrangian simulation of flamelet extinction and re-ignition in turbulent jet diffusion flames. *23rd Symposium (Int'l.) on Combustion.* The Combustion Institute, Pittsburgh, 693-698.

MILLER, J. A. & BOWMAN, C. T. 1989 Mechanism and modeling of nitrogen chemistry in combustion. *Prog. Energy Combust. Sci.* **15**, 287-338.

NISHIOKA, M., NAKAGAWA, S., ISHIKAWA, Y. & TAKENO, T. 1994 NO emission characteristics of methane-air double flame. *Combust. Flame* **98**, 127-138.

PETERS, N. & DONNERHACK, S. 1981 Structure and similarity of nitric oxide production in turbulent diffusion flames. *18th Symposium Int'l. on Combustion,* The Combustion Institute, Pittsburgh, 33-42.

POPE, S. B. & CORREA, S. M. 1986 Joint PDF Calculations of an Non-Equilibrium Turbulent Diffusion Flame. *21st Symposium (Int'l.) on Combustion,*The Combustion Institute, 1341-1348.

SAMANIEGO, J.-M., EGOLFOPOULOS, F. N. & BOWMAN, C. T. 1995 CO_2^* Chemiluminescence in Premixed Flames. *Combustion Science and Technology* **109**, 183-203.

SAMANIEGO, J.-M., LABÉGORRE, B., EGOLFOPOULOS, F. N., DITARANTO, M., SAUTET, J.-C. & CHARON, O. 1996 Mechanisms of Nitric Oxide Formation in Oxygen-Natural Gas Combustion. *In preparation.*

TAKENO, T., NISHIOKA, M. & YAMASHITA, H. 1993 Prediction of NOx emission index of turbulent diffusion flame. In *Turbulence and Molecular Processes in Combustion,* Elsevier Science Publishers B. V., Amsterdam, 375-392.

TURNS, S. R. & MYRH, F. H. 1991 Oxides of nitrogen emissions from turbulent jet flames: Part I-fuel effects and flame chemistry. *Combust. Flame* **87**, 319-335.

VERVISCH, L. 1992 Study and modeling of finite rate chemistry effects in turbulent non-premixed flames. *Annual Research Briefs*, Center for Turbulence Research, Stanford Univ./NASA Ames, 411-429.

VRANOS, A., KNIGHT, B. A., PROSCIA, W. M., CHIAPETTA, L. & SMOOKE, M. D. 1992 Nitric oxide formation and differential diffusion in a turbulent methane-hydrogen diffusion flame. *24th Symposium (Int'l.) on Combustion.* The Combustion Institute, Pittsburgh, 377-384.

WILLIAMS, F. A. 1985 *Combustion Theory*, Benjamin/Cummings, Menlo Park.